


Original Research

Redox treatment ameliorates diabetes mellitus-induced skin flap necrosis via inhibiting apoptosis and promoting neoangiogenesis

Yeon S Kim¹, Hye-Young Lee², Jeon Y Jang², Hye R Lee², Yoo S Shin²  and Chul-Ho Kim²

¹Department of Otorhinolaryngology, College of Medicine, Konyang University Hospital, Konyang University, Daejeon 35365, Korea;

²Department of Otolaryngology, School of Medicine, Ajou University, Suwon 16499, Korea

Corresponding author: Yoo S Shin. Email: ysshinmd@ajou.ac.kr

Impact statement

Diabetes causes a lot of complications, especially in the process of wound healing in diabetic patients. In spite of many studies, the treatment for diabetic wounds is not yet sufficient. Edaravone (EDV) can suppress oxidative stress through scavenging free radicals. Since the wounds of diabetic patients are caused by oxidative stress, we hypothesized that EDV will help in the recovery of diabetic wounds. This study investigates whether EDV can reduce oxidative stress in wound healing HaCaT/human dermal fibroblasts cells (HDFs) *in vitro* and *in vivo*. EDV protects HaCaT/HDFs against H₂O₂-induced cellular injury via inhibiting early apoptosis and inflammation; moreover, EDV encourages the wound healing of diabetic rats by promoting neoangiogenesis. These results suggest the possibility that EDV could be great help in the recovery of oxidative stress induced wounds in diabetic patients.

Abstract

Intractable wound healing is the habitual problem of diabetes mellitus. High blood glucose limits wound healing by interrupting inflammatory responses and inhibiting neoangiogenesis. Oxidative stress is commonly thought to be a major pathogenic cause of diabetic complications. Edaravone (3-methyl-1-phenyl-2-pyrazolin-5-one, EDV) is a free radical scavenger which suppress oxidative stress. This study investigates whether EDV can reduce oxidative stress in wound healing HaCaT/human dermal fibroblasts cells (HDFs) *in vitro* and *in vivo* animal model. Cell viability and wound healing assays, FACS flow cytometry, and Hoechst 33342 staining were performed to confirm apoptosis and cytotoxicity in H₂O₂ and EDV-treated HaCaT and HDFs. A streptozotocin-induced hyperglycemic animal model was made in adult C57BL6 mice. Full-thickness skin flap was made on dorsomedial back and re-sutured to evaluate the wound healing process. EDV was delivered slowly in the skin flap with degradable fibrin glue. The flap was monitored and analyzed on postoperative days 1, 3, and 5. CD31/DAPI staining was done to detect newly formed blood vessels. The expression levels of NF- κ B, bcl-2, NOX3, and STAT3 proteins in C57BL6 mouse tissues were also examined. The wound healing process in hyper- and normoglycemic mice showed a difference in protein expression, especially in oxidative stress management and angiogenesis. Exogenous H₂O₂ reduced cell viability in a proportion to the

concentration via apoptosis. EDV protected HaCaT cells and HDFs from H₂O₂ induced reactive oxygen species cell damage and apoptosis. In the mouse model, EDV with fibrin resulted in less necrotic areas and increased angiogenesis on postoperative day 5, compared to sham-treated mice. Our results indicate that EDV could protect H₂O₂-induced cellular injury via inhibiting early apoptosis and inflammation and also increasing angiogenesis. EDV might be valuable in the treatment of diabetic wounds that oxidative stress has been implicated.

Keywords: Chronic wounds, diabetes mellitus, edaravone, oxidative stress, reactive oxygen species

Experimental Biology and Medicine 2021; 246: 718–728. DOI: 10.1177/1535370220974269

Introduction

Diabetes mellitus (DM) is a chronic disease with a high prevalence worldwide.¹ Failure of wound healing due to diabetes is a frustrating challenge for clinicians. When a wound develops there are four steps to recovery: hemostasis, inflammation, proliferation, and tissue remodeling. The inflammation phase consists of homeostasis and inflammation. It is then followed by a proliferative phase

with granulation, contraction, and epithelialization. In DM wound healing, the inflammation stage commonly lasts long and the wound became chronic and does not heal because of the imbalance between producing and degrading collagen.² The remodeling phase includes forming of cellular connective tissue, collagen maturation, and capillary pruning.³ Insufficient angiogenesis plays a critical role in the etiology of diabetic wound healing.⁴ Continuing inflammatory cascade leads to result in an increase in

tissue destruction rather than healing. Long-lasting inflammation is a frequent complication in diabetic wound healing. In the process of DM, wound healing is impaired due to abnormal neovascularization. In the chronic diabetic wounds, healing process is very difficult due to insufficient blood supply and local edema. In addition, current treatment options are limited and inefficient. Different drugs and delivery systems targeting the wound healing process of diabetic patients have been reported, but the results have not been satisfactory.⁵ Thus, new therapeutics should be developed to satisfy unmet clinical needs.

Although reactive oxygen species (ROS) generation is ordinary physiological reactions, oxidative stress is triggered by an unbalance between the generation and elimination of ROS. ROS are necessary for defending against pathogenesis and helping successful cellular recovery during wound healing. However, if ROS are excessively produced or not properly cleansed, they could cause oxidative stress and cause cellular damage. The level of ROS increased in chronic non-healing wounds in DM.⁶ Excessive ROS is reported to degrade extracellular matrix proteins.⁷ Therefore, maintaining adequate levels of ROS play an important role to promote wound recovery. In diabetic microvasculature, ROS overproduction might impair angiogenesis and result in delayed wound healing or cell death.⁶ Edaravone (3-methyl-1-phenyl-2-pyrazolin-5-one, EDV) used in the treatment of acute cerebrovascular diseases as an antioxidant.⁸ EDV can reduce the increased amount of ROS induced by post-ischemic reperfusion. EDV could promote wound healing through its ability of scavenging free radical which concerned as a pathogen in DM. Thus, we expect that EDV could be a promising medicine for failure of wound healing due to oxidative stress. To date, only a few reports about this possibility have been reported.

The objectives of this study were to evaluate ROS generation and apoptosis of H₂O₂ upon human dermal fibroblasts (HDFs) and HaCaT cells, to determine the effects of EDV on oxidative stress-induced cell damage and to confirm that EDV has healing effect in a DM mouse wound model and elucidate the underlying mechanism of these effects. This study investigated whether the topical application of EDV could accelerate healing process in the wound of diabetic mice via neovascularization.

Materials and methods

Cell maintenance

Human dermal fibroblast was isolated from foreskin of patients who have received informed consent for use of residual tissue for academic research which was approved by the Institutional Review Board of Ajou University Hospital (AJIRB-GEN-GEN-12-107) and processed according to human ethics guidelines. Cell maintenance was done as previously described.^{9,10} Normal human HaCaT keratinocytes and HDFs were grown in Dulbecco's modified Eagle's medium (DMEM, Welgene, Daegu, Korea) with 10% fetal bovine serum (FBS, Gibco, USA) and 1% antibiotics. Cells were dissociated from cell culture surface using

0.05% Trypsin/0.02% EDTA (Invitrogen, USA) and were used from passages 2 to 5.

Cell viability assay

Cell viability assay was done as described previously.^{11,12} In 100 ϕ dishes, HaCaT and HDF were cultured for one week under normal recommended condition (4.5 mg/mL D-glucose) and high glucose concentration (9.0 mg/mL D-glucose, Sigma-Aldrich., USA) conditions, respectively. Hyperglycemic glucose concentration was prepared by adding D-glucose to cell maintenance DMEM.

To investigate the effects of EDV (Sigma-Aldrich, USA) on cell growth in different glucose concentrations, after H₂O₂ treatment with or without EDV treatment cell viability was measured using an EZ-cytox assay (Daeil Lab Service Co, Seoul, Korea). At 24 h after treatment, the cells were mixed with 100 μ L of EZ-Cyto X solution and incubated at 37°C for 1 h. Cell viability was determined after measuring the absorbance at 450 nm using an enzyme-linked immunosorbent assay (ELISA) reader (Bio-Tek, Winooski, VT, USA). All results are stated as mean percentage \pm standard deviation (SD) of four independent experiments. When comparing treatment group and control group, statistically significant differences were measured when the *P*-value was less than 0.05 as determined by the Student's *t*-test.

Fabrication of fibrin hydrogel and indirect assessment of cell death

Fibrinogen stock solution (40 mg/mL) was prepared by dissolving lyophilized bovine blood plasma protein (Millipore, USA) at 37°C with 1% bovine serum albumin in sterile Dulbecco's phosphate-buffered saline (DPBS, Welgene, Daegu, Korea). A stock solution of thrombin was prepared by reconstituting thrombin at 5 U/mL using sterile DPBS, which was then stored at -20°C in a microtube. Fibrin hydrogels were produced with pre-warmed fibrinogen solution and crosslinked with thrombin. To allow the gelation process, hydrogels were incubated at 37°C for 30 min in a humidified atmosphere. The final fibrinogen concentration was 2 mg/mL.

To create fibrin with EDV hydrogels, EDV was dissolved in ethanol at concentrations of 200 mM. Fibrinogen was mixed with EDV to the specified concentration. Fibrin-EDV hydrogel samples were soaked in serum-free DMEM at 37°C in a humidified atmosphere. At pre-determined time intervals, the supernatant was collected and replaced by the same volume of fresh serum-free DMEM. The next day after cells were seeded at a density of 1×10^4 cells/well in 96-well plate, the culture medium was replaced with EDV released serum-free DMEM. Cytotoxic effects of EDV on HDFs and HaCaT treated with or without H₂O₂ were then evaluated. After each treatment, 10 μ L of EZ-Cyto X solution was applied to each well. After 1 h incubation, the absorbance was measured at 450 nm using an ELISA reader (Bio-Tek) and corrected by subtracting the background signal from a well containing only 100 μ L DMEM with 10% FBS.

Wound healing assay

Wound healing assay was done as reported before.¹³ Cells were seeded on 24-well plates and then grown to confluence. A wound was made by scratching with a pipette tip within a cell monolayer. Cell migration was analyzed after 24 h. At 0 to 24 h time points, cells were fixed with 4% paraformaldehyde for 10 min and stained with 1% crystal violet for 10 min. Cell migration image was taken with an EVOS FL Auto 2 live-cell imaging system (EVOS2, Thermo Fisher Scientific, USA).

ROS scavenging assay

This assay was conducted as previously described.¹⁴ Intracellular ROS scavenging assays were done by measuring the dihydroethidium (DHE) fluorescence intensity which was proportionally increased according to the amount of ROS. Cells treated with or without EDV were incubated with H₂O₂ for 24 h before harvesting. They were mixed with DHE solution and incubated at 37°C for 1 h. The fluorescence intensity was measured using EVOS2.

Analysis of cell apoptosis by FACS

FACS analysis was conducted as previously described.¹⁵ Cell apoptosis were measured by assessing the incorporation of propidium iodide (PI), a fluorescent dye. Cells pretreated with and without EDV and H₂O₂ were collected, resuspended, and then stained with PI and Annexin V. Fluorescence intensity was measured by using a BD FACS flow cytometer (Thermo Fisher Scientific).

Streptozotocin-induced diabetic mouse model and skin flap design

Diabetic animal model and skin flap experiment were conducted as previously described.¹⁶ The protocol for animal studies was approved by the Ethics Committee for Animal Care and Use (No.2017-0025), Ajou University, Suwon, Republic of Korea.

Comparison of normoglycemia and hyperglycemia of random skin flap. The C57BL6 mice (20–25 g, six weeks old, Orient Bio Co., Korea) were distributed into two groups. Each group consisted of 15 mice in the beginning study. Control group mice were non treated as normoglycemia and other 15 mice were intraperitoneally injected 6 weeks of age with 40 mg/kg of streptozotocin (STZ, Sigma-Aldrich) daily for 5 days to induce hyperglycemia. All mice were housed (3–4 animals/cage) under a 12 h light-dark cycle and were fed a standard rodent diet with water. Blood glucose level was measured with GlucoDr Plus (Allmedicus, Korea). After four weeks, only the mice with glucose level above 250 mg/dL were used in this experiment.

Hyperglycemia mice skin flap with hydrogel. In this study, 30 male C57BL6 mice with STZ-induced hyperglycemia were randomly assigned to 10 mice. Four weeks post-STZ, 1.5 × 3.0 cm random skin flap was made on the dorsal side of the mice, and sutured original position.

Concentrated fibrinogen solution (with/without EDV) and thrombin were same volumes loaded into each syringe and were injected. The hydrogel was injected into sutured skin flap pocket.

Skin flap surgical procedures

Skin flap procedure was done as previously described.¹⁷ Animals were anesthetized by allowing them to inhale 4% isoflurane in a glass chamber. The mice were then shaved at the dorsal area and a random skin flap 1.5 × 3.0 cm in size was made on each mouse using surgical scissors. The skin flap was sutured using 4-0 silk in the original position.

Measurement of the necrotic area of skin flap

We measured the necrotic area of skin flap as described previously.¹⁸ Dorsal skin flaps were photographed and recorded with a digital camera (D90, Nikon, Japan) on postoperative days 1, 3, and 5. The necrotic area was defined as the presence of scab formation, alopecia, loss of elasticity. The proportion of necrotic area of the total flap area was calculated by ImageJ software (NIH, USA).

At postoperative day 5, flap survival was estimated by measuring sizes of viable and ischemic areas using image analysis. Photographs of the flaps at the same distance and focus were taken. Results are expressed as percentages of survival area relative to the total flap surface area. The viable tissue was demarcated grossly in a blinded fashion based on its texture, color, and appearance by two independent observers. The survival area was calculated in square centimeters using ImageJ software.

Western blotting analysis

Western blotting was conducted as described previously.¹⁹ Cells were placed on a 10-cm dish and received treatments for 24 h. To isolate proteins, cultured cells were washed with cold PBS and resuspended in lysis buffer (RIPA buffer, Sigma-Aldrich) in the presence of protease inhibitor cocktail (Roche Molecular Biochemicals). Tissue samples (dia 8 mm) from the intermediate of flap area were also harvested and homogenized. After incubation on ice for 30 min and centrifugation at 12,000g for 15 min at 4°C, the supernatant was collected. Protein concentration was determined using the Bradford method. Samples containing equal amounts of protein were then subjected to Western blotting. Proteins were separated by 10% polyacrylamide gel electrophoresis and electrophoretically transferred to polyvinylidene fluoride membrane. The membranes were blocked with 5% skim milk in TBS-T buffer and subsequently with the appropriate primary antibodies diluted 1:1000 against cyclooxygenase (COX)2 (Cell signaling, 12282), nicotinamide adenine dinucleotide phosphate oxidase (NADPH oxidase, NOX) 3 (Sigma, SAB4502060), TNF- α (Santa Cruz, sc-8301), phospho-STAT3 (Cell signaling, 9145), STAT3 (Cell signaling, 4904), phospho-nuclear factor κ B (NF- κ B) (Cell signaling, 3033), NF- κ B (Cell signaling, 4764), Bcl-2 (Santa Cruz, sc-7382), and GAPDH (Cell signaling, 2118) at 4°C for overnight.

After washing with TBS-T, membranes were incubated with horseradish peroxidase-conjugated secondary antibodies anti-mouse (7076S) and goat anti-rabbit (7074S) HRP-conjugated IgGs were purchased from Cell Signaling Technology for an hour (1:5000 dilution). Then immunoreactive proteins were visualized by chemiluminescence detection system (Amersham Biosciences, Little Chalfont) and imaged by LAS 3000 Bio Imaging Analysis System (Fuji Film). The relative intensity of the western blot band was quantified using ImageJ (National Institutes of Health, NIH) densitometry software (mean \pm SD of three independent experiments).

Hematoxylin and eosin staining

H&E staining was done as described previously.²⁰ After animals were euthanized, skin specimens were rinsed with PBS for 5 min and then fixed with 4% paraformaldehyde at 4°C overnight. Specimens were cryoprotected with 30% sucrose in PBS at 4°C overnight and embedded with OCT compound. H&E staining was done on 6 μ m-thick sections mounted on poly-L-lysine-coated slides. Using EVOS2 under \times 200 magnification, four randomly selected fields of neutrophils were evaluated in four random sections. The number of neutrophils per area (mm²) was calculated

Immunofluorescence (CD31) staining

Immunofluorescence (CD31) staining was performed as described previously.²¹ Tissues were cut into 6 μ m thick using a cryostat and collected on poly-L-lysine-coated slides. After rehydration, the blocking of specific antibody activity was performed by preincubating with 5% goat serum and 0.025% Triton X-100 in PBS for 1 h, and first incubated with primary antibody, hamster anti-CD31 (Millipore, MAB1398Z) diluted 1:100 in PBS containing 1% bovine serum albumin, at 4°C overnight in a dark slide tray and then incubated in secondary antibody. The secondary antibody for immunofluorescent staining was conjugated with CyTM 3 (goat anti-American hamster IgG, 127-165-160, Jackson ImmunoResearch Laboratories, USA). For nuclear staining, samples were incubated for 2 min in 4',6-diamidino-2-phenylindole (DAPI; D9542, Sigma-Aldrich) diluted 1:1,000 in PBS. Image analysis was then performed with an EVOS2.

Statistical analyses

The data in each experimental group were expressed as means \pm standard deviations. Significance was determined by using one-way analysis of variance (ANOVA) with the GraphPad Prism version 7.0. A *P*-value less than 0.05 was regarded statistically significant.

Results

The wound healing process in hyper- and normoglycemic mice showed a difference in protein expression

To determine the possible pathogenic mechanism of wound failure in hyperglycemic mice, skin flaps were made on the back of hyper- and normoglycemic mice and the size of

necrotic area and skin thickness was compared in both groups. The necrotic area was larger and the skin was thinner in hyperglycemic mice than in normoglycemic mice (Figure 1(a) and (b)). H&E and CD31 fluorescence staining revealed that in normoglycemic mice, more neovascularization was observed than in STZ-induced hyperglycemic mice (Figure 1(c) and (d)). Western blot analysis was done using tissue to compare the difference between normo- and hyperglycemic mice. In hyperglycemic mice, the expression of COX2 and NF- κ B on postoperative day 5 was significantly increased. NOX3, STAT3, and TNF- α levels were also changed, even though the difference was not statistically significant (Figure 1(e)). COX2 is an enzyme induced by external stimuli. It plays a crucial role in the expression and progression of various degenerative diseases including inflammation and cancer. NF- κ B targets inflammation by directly increasing the production of inflammatory chemokines and cytokines, and by regulating cell proliferation, apoptosis, and differentiation. Therefore, we focused on redox treatment for hyperglycemic skin flap wound healing.

EDV protects HaCaT and HDFs from H₂O₂-induced ROS damage and apoptosis

Cell viability was compared after treatment with H₂O₂ or EDV at control and high glucose concentration conditions in both HaCaT cells and HDFs. When the cells were treated with increasing doses of H₂O₂ in control conditions for 24 h, survival decreased with increasing concentrations of H₂O₂ as shown in Figure 2(a). To investigate whether EDV could confer protection against H₂O₂-induced cell damage in HaCaT cells and HDFs, cell viability was measured after incubating with various concentrations of EDV (10 to 1000 μ M) for 24 h. Our results showed that treatment with EDV prevented the decrease in cell viability induced by H₂O₂ in a dose-dependent manner. When the same test was repeated in high glucose concentration conditions with glucose concentration at 9.0 mg/mL, the decrease in cell viability by H₂O₂ was more pronounced, but recovery after EDV treatment was also observed (Figure 2(a)). DHE fluorescence was measured to see changes in ROS levels caused by 0, 100, and 500 μ M of H₂O₂ after treatment with or without 100 μ M EDV. After EDV treatment, the amount of ROS was significantly decreased in HDFs and HaCaT cells (Figure 2(b)). The migration of HaCaT cells and HDFs was also decreased after treatment with H₂O₂. Cell migration was increased after treatment with EDV (Figure 2(c)). Apoptotic levels were quantified by flow cytometric analysis to measure the extent of H₂O₂-induced apoptosis and to evaluate whether EDV could protect against the apoptosis. HaCaT cells and HDFs were treated with different concentrations of H₂O₂ (0–1000 μ M) with or without EDV (50–200 μ M) for 24 h. As shown in Figure 2(d), the amount of apoptotic cells increased with the increase of the concentration of H₂O₂. According to our experiment results, EDV treatment significantly (*P* < 0.05) reduced the rate of apoptosis induced by H₂O₂ (Figure 2(d)). Hoechst 33342 staining showed an increase in apoptotic morphology represented by chromatin condensation and nuclear shrinkage after increasing concentration of H₂O₂ treatment from 100 μ M to 500 μ M.

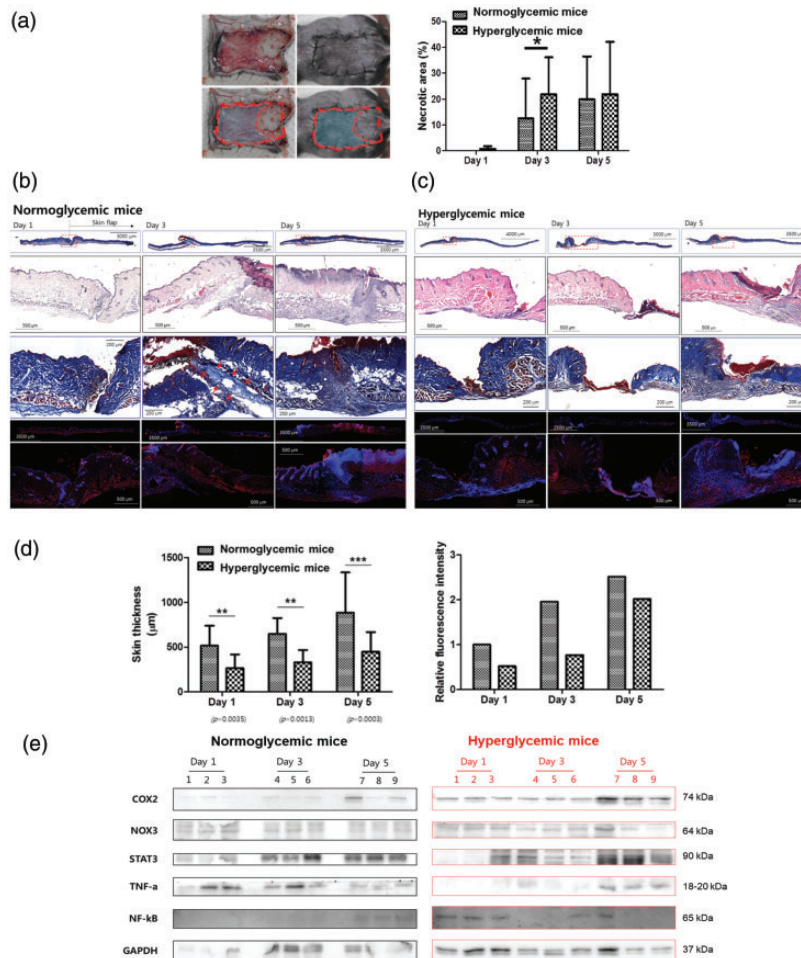


Figure 1. Wound healing in normo- and hyperglycemic mice. (a) Full-thickness wounds were created on the backs of control and streptozotocin-induced hyperglycemic mice. The wounds were examined one, three, and five days after wound creation. The extent of the difference in the necrotic area (%) between normo- and hyperglycemic mice model. (b, c) H&E and CD31-stained representative sections of (b) normoglycemic mice and (c) hyperglycemic mice wound harvested one, three, and five days after wound creation. (d) The quantification of skin thickness (μm) and relative fluorescence intensity of normoglycemic and hyperglycemic mice one, three, and five days after wound creation. (e) The expression of COX2, NOX3, STAT3, TNF- α , and NF- κB was calculated in normoglycemic and hyperglycemic mice examined one, three, and five days after wound creation. Measurements were made in duplicate in three mice in each group and each day. Western blots are representative of three different experiments. Results are expressed as mean \pm SD. (A color version of this figure is available in the online journal.)

In cells treated with $500 \mu\text{M}$ H_2O_2 , normal nuclear morphology was hardly found. However, treatment with $100 \mu\text{M}$ EDV reduced the apoptotic fraction of cells (Figure 2(e)). Taken together, these findings suggest that EDV is capable of attenuating H_2O_2 -induced ROS formation and cell apoptosis.

Topical application and controlled delivery of EDV can accelerate wound healing in hyperglycemic mice in vivo

Effects of EDV were evaluated on the healing of full-thickness wounds on the backs of STZ-induced diabetic mice. Vehicle control, fibrin only, and EDV with fibrin were applied after wound creation. Digital wound images of each group from days 1, 3, and 5 are presented in Figure 3(a). Wound healing effects of EDV with fibrin were estimated by calculating the necrotic area (%) (Figure 3(a)) and neutrophils/area (%) (Figure 3(b)) after measuring the wound area. In the group treated with EDV and fibrin, both the necrotic and neutrophilic areas

were significantly smaller than in other groups. We found that the wound neutrophilic area of EDV with fibrin was almost one-fifth that of untreated diabetic wounds. The wound area was tracked histologically for one, three, and five days. On post-wounding day 5, EDV-loaded fibrin gel significantly accelerated the repair of wounds in the diabetic model (Figure 3(c) and (d)). CD31/DAPI staining indicated that more abundant blood vessels were observed in the wound sites of the EDV with fibrin-treated group than in the control wound sites. EDV promoted neovascularization in diabetic wounds (Figure 3(c), yellow arrows). As presented in Figure 3(e), the expression levels of p-STAT3, STAT3, NOX3, p-NF- κB , NF- κB , and bcl-2 were confirmed in the tissues of mice by Western blotting. bcl-2 expression was increased over time in EDV with fibrin-treated mice. In addition, the expression levels of STAT3 and NF- κB were reduced (Figure 3(e)). These results indicate that inflammation was reduced and cell apoptosis was suppressed in the EDV-treated group.

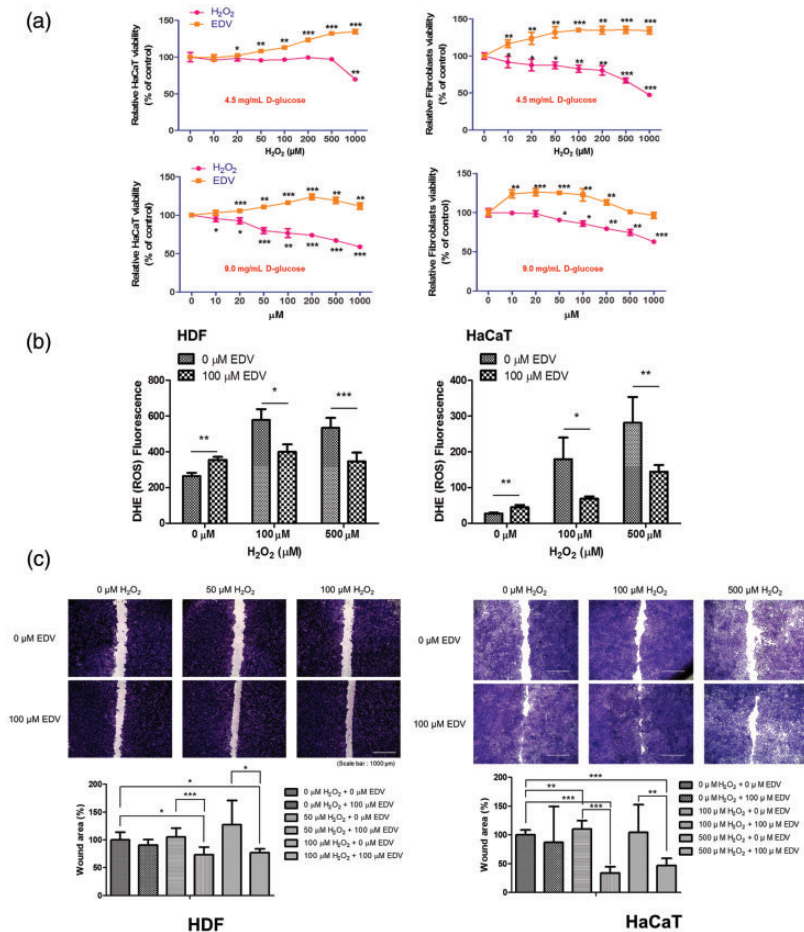


Figure 2. The protective effect of edaravone on H_2O_2 -induced cell injury. (a) The HDF and HaCaT cells viability with or without EDV after treated with 0–1000 μM H_2O_2 in control (4.5 mg/mL D-glucose) and high glucose concentration (9.0 mg/mL D-glucose) conditions for one week. (b) The compartment of dihydroethidium cellular reactive oxygen species detection in HDFs and HaCaT cells with or without 100 μM EDV treatment after treated with 0–500 μM H_2O_2 . (c) Wound healing assay of HaCaT cells and HDFs with or without EDV treatment after H_2O_2 induced ROS generation. (HaCaT cells; $n=6$, HDFs; $n=6$) The data were analyzed using a one-way ANOVA followed by post hoc Tukey's multiple comparison tests. * $P < 0.05$, ** $P < 0.01$, *** $P < 0.001$. (A color version of this figure is available in the online journal.)

Discussion

In diabetes, the greatest difficulty in the process of wound healing is mainly due to persistent oxidative stress. Even though ROS plays essential roles in diverse cellular events, excessive oxidative stress might interfere with normal physiologic inflammatory reactions during wound healing. Several components of ROS, such as the H_2O_2 used in this study, may lead various oxidization initiating subsequent cell deaths or cellular damages. Oxidative stress is considered a major risk factor that exacerbates wound damage via different molecular pathways especially in DM.^{6,22,23} Therefore, eliminating excessive ROS or preventing their generation by ROS scavengers that can counteract ROS-induced cell death may be effective in preventing the degeneration of wounds in DM. Topical applications of redox material such as EDV could accelerate the healing of diabetic wounds by decreasing oxidative damage. In the present study, we presented EDV with fibrin gel as a potential efficient treatment material for wound healing in diabetes.

Our results provide proof of EDV protection against H_2O_2 -induced cellular injury in high glucose concentration conditions. H_2O_2 treatment decrease viability of cell in a

concentration dependent manner. EDV treatment successfully restored cell viability. According to the results of cell viability decrease, we identified cell apoptosis in response to the generation of ROS. Exposure of H_2O_2 to HaCaT cells and HDFs increases apoptosis and ROS levels. Conversely, treatment of cells with EDV reduces both the apoptotic rate and the production of ROS generation in both types of cells. These protective effects might be due to the redox activity of EDV. After discovering that EDV display a protective effect on H_2O_2 induced cytotoxicity, we also studied these effects in an established diabetic environment. As shown in our experiments, EDV could protect HDFs and HaCaT cells from H_2O_2 induced cell apoptosis in a high glucose concentration environment, indicating the possibility that it may be effective in the treatment of a diabetic wound. The effects of EDV on wound recovery were also confirmed in a full-thickness wound model in mice with STZ-induced DM. While doing *in vivo* experiments with, we measured recovery potential by comparing specimens. In EDV-loaded fibrin gel treated mice, the necrotic area (15%) was less than half that of the control (30%) at five days after treatment. More neovascularization was also observed in the EDV-fibrin gel-treated group than others. In our

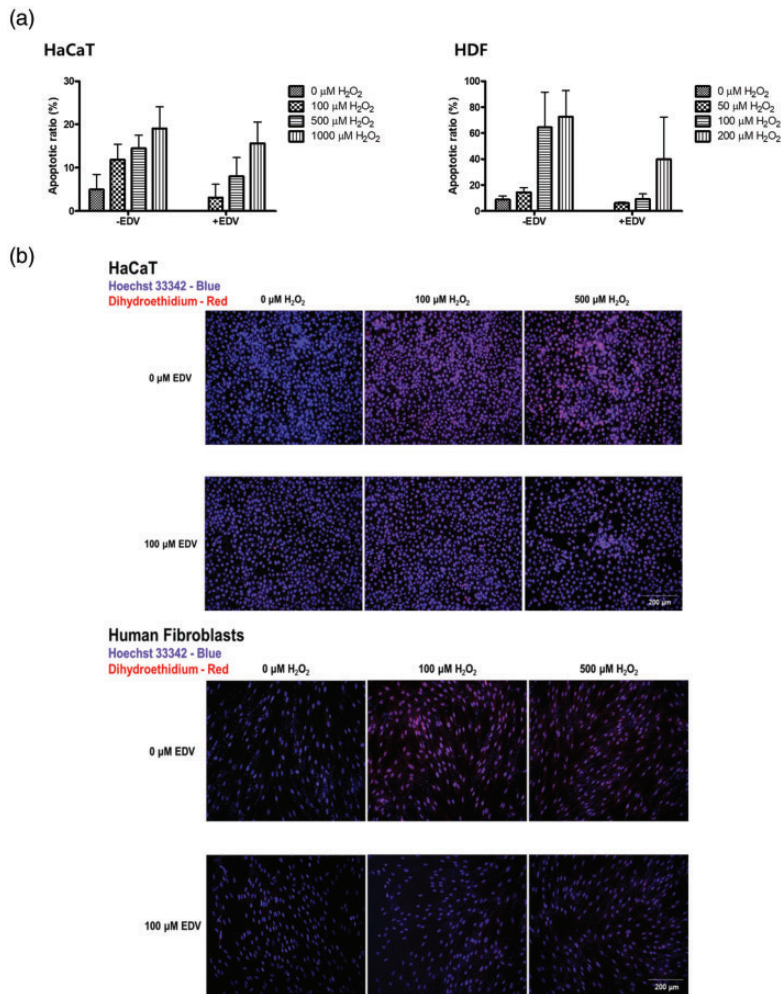


Figure 3. The protective effect of edaravone on H_2O_2 -induced cell apoptosis. (a) Cell apoptosis was assessed by flow cytometry. FACS analysis of HaCaT cells and HDFs with or without EDV treatment after H_2O_2 induced ROS generation by concentration. (b) Hoechst 33342 and DHE of HaCaT cells and HDFs with or without EDV treatment after 0, 100, 500 μM of H_2O_2 induced ROS generation. The data were analyzed using a one-way ANOVA followed by post hoc Tukey's multiple comparison tests. * $P < 0.05$, ** $P < 0.01$, *** $P < 0.001$. (A color version of this figure is available in the online journal.)

experiments, we found that the topical application and controlled release of EDV from fibrin gel helped heal the wounds of diabetic mice.

Hyperglycemia damages the microvasculature that carries oxygen and nutrients to wound, which causes wound healing problem.²⁴ Excess glucose thickens the wall of endothelial cell and slows blood flow, preventing the movement of erythrocytes, which are essential for tissue recovery.²⁵ Deveci *et al.* showed that hyperglycemia induced apoptosis in keratinocytes.²⁶ Xuan *et al.* provided high-glucose concentration environment to human fibroblast and evaluated the molecular mechanism of hyperglycemia on healing process.²⁷ They show that hyperglycemia increases the production of ROS resulting in impaired wound healing²⁷ and inhibits human fibroblast migration.²⁷⁻²⁹ In this investigation, we measured the difference between wound thickness through tissue staining and fluorescence transmittance. Wounded hyperglycemic mice experienced more severe necrosis than normoglycemic mice and the thickness of the recovered skin was thinner in hyperglycemic mice. This impaired wound healing might be attributed to excessive ROS because proteins

related to redox were less expressed in the hyperglycemic mice than in the control. By combining the result of our experiments with past publications, we focused on a redox treatment strategy using EDV for DM wound healing.

EDV is a free radical scavenger which decrease neurological damage in cerebrovascular ischemia.^{30,31} EDV has been verified to be a capable treatment material to scavenge ROS and to prevent lipid peroxidation.³¹ It has also been known to be effective in inhibiting inflammatory responses³² and oxidative tissue damage.³⁰ Lately, EDV has been offered as a feasible treatment for oxidative stress-induced degenerative diseases, such as heart attack,³³ stroke,³⁴ and diabetes.^{35,36} The underlying treatment mechanism of EDV effect is via inhibiting oxidative stress, following a reduced inflammatory response, and thereby prevents cell death. However, studies on its effect and treatment mechanisms are lacking. In this experiment, we aim to verify the redox role of EDV in a DM wound healing animal model. Moreover, another mechanism by which EDV may be effective in wound healing is in promoting neovascularization, which includes angiogenesis

(new vessels made from preexisting vessels) and vasculogenesis (new vessels need both preexisting blood vessels and endothelial progenitor cells).³⁷ Naito *et al.* report that EDV modulates angiogenesis by increasing nitric oxide production in diabetic wounds.³⁸ These results were consistent with a study by Koizumin *et al.* who observed that EDV is effective against burn injury with extensive ROS production.³⁹

Our principal proposal is that EDV can promote neovascularization in wounds of diabetic mice. Neovascularization occurs by quenching ROS in wounds, leading to more rapid wound healing. Hoeldtke *et al.* described that superoxide which contributed to a reduction in NO bioavailability and an inhibition of wound healing was increased in STZ-induced diabetic mice.⁴⁰ As with that research results, we found that EDV accelerated wound healing in DM by increasing neovascularization.

As shown in Figure 1, we compared the changes in TNF- α , NF- κ B, COX2, NOX3, and STAT3 in the tissue of wound after confirming that more necrosis occurred and the recovered expression of TNF- α , which contributes to diabetic microvascular complications⁴¹ by regulating glucose metabolism and inhibiting insulin secretion in pancreatic beta cells.⁴² During the wound healing process, macrophages are divided into M1 and M2. TNF- α is a cytokine secreted from M1 macrophage and induces cell apoptosis through oxidative stress.⁴³ The amount of TNF- α expressed through our data varies depending on the amount of glucose in mice. Hyperglycemia leads to the production of ROS, which induce the activation of the NF- κ B, inflammatory cytokines, and chemokines directly.^{44,45} NF- κ B targets inflammation directly by increasing the creation of inflammatory molecules, also in regulating cell proliferation, apoptosis, and differentiation. Similar to the previous results, in our experiment results, NF- κ B showed a tendency to increase in hyperglycemia. We could predict that decreasing the level of NF- κ B decreases inflammation and promotes wound healing.

COX2 is an inducible enzyme expressed by external stimuli such as ROS, and it plays an essential role in the expression and progression of various diseases. The up-regulation of NOX causes the development of pathophysiological oxidative stress. Increased ROS in wounds through hyperglycemia-mediated COX and NOX activation results in the oxidative stress that induces impaired wound healing.

In our experiments, TNF- α , NF- κ B, COX2, NOX3, and STAT3 were all increased as the days passed in wounds of hyperglycemia mice. In normoglycemia mice, COX2 and STAT3 increased with time, but there was no significant difference between TNF- α and NF- κ B, and NOX decreased slightly. This may explain that hyperglycemic mice show more inflammation and take longer time in the recovery process after wounding than normoglycemic mice.

In another animal experiment, the role of EDV in the wound healing of skin flaps was evaluated (Figure 4). When EDV with fibrin hydrogel was treated on hyperglycemic mice wounds, the expression level of p-STAT3, STAT3, NOX3, NF- κ B was decreased, and there was no significant difference in p-NF- κ B, and bcl-2 showed a

tendency to increase in Western blot analysis. As revealed in the previous experiment, STAT3, NOX3, and NF- κ B are proteins that aggravate inflammation by increasing hyperglycemia-induced ROS. We expected that as the NF- κ B increased in hyperglycemia was reduced by EDV, its active form, p-NF- κ B would also decrease further, but the experimental results did not show any significant decrease.

According to our study, diabetic mice had a higher initial STAT3 expression than normal mice. According to recent research, it is indicated that hyperglycemia increases the activity of STAT3 known as a cytoplasmic transcription factor and contributes to the pathophysiology of poor wound healing.⁴⁶ Overexpression of STAT3 causes inflammation that delay in wound healing and increases atopic dermatitis through the STAT signaling pathway. After EDV treatment, diabetic mice showed decreased phosphorylation of STAT3. Bcl-2 was considered to be related to the anti-apoptotic effect of EDV. In the wounds of diabetic mice, early phase cell apoptosis is increased, while bcl-2 level is decreased compared to those in normal mice.⁴⁷ EDV treatment increased bcl-2 levels in diabetic mice and resulted in antiapoptotic effects. In the present study, the anti-inflammatory effect of EDV on diabetic wounds was evaluated in mice.

To deliver EDV on the targeted area in a suitable spatio-temporal manner and to create a favorable regenerative environment, we chose fibrin glue. Fibrin, a naturally derived scaffold hydrogel, is the final by-product of the blood coagulation process. Fibrin not only promotes wound healing by directly affecting cellular actions, but also acts as a delivery system that controlled releases therapeutic molecules. In preclinical experiments, fibrin hydrogels have been used as a platform to deliver various cells including fibroblasts⁴⁸ and mesenchymal stem cells,^{49,50} various genes,^{51,52} and drugs to the target area. Fibrin hydrogels have many advantages due to high-water content, biocompatibility, and biodegradability.⁵³ Fragment E, a byproduct of fibrin, is known to stimulate angiogenesis and cellular migration.⁵⁴⁻⁵⁶ Angiogenesis is a key process in wound recovery, and fibrin and its by-products induce vascular endothelial growth factor secretion, thereby causing angiogenesis.⁵⁶ The role of the fibrin-based drug is to mix the pharmaceutically active drug with the fibrinogen thrombin formula and apply it to the site of injury so that the drug slowly and consistently releases its effects. Various clinical indications such as large severe burns, trauma injury, and chronic DM wounds, which have persistent infections, require localized, high-dose delivery of pharmaceuticals such as in fibrin-based formulation. The reason for using EDV and fibrin formulations is to improve bioavailability and to offer controlled release of EDV, which is definitely great value to provide EDV for a prolonged period of time to advance DM wound healing.

The conclusion of our study is that EDV with fibrin hydrogel may be effective in promoting recovery in diabetic wounds. EDV with fibrin works on DM wound healing by inhibiting early apoptosis via increasing bcl-2 while decreasing STAT3 and NF- κ B to suppress inflammation and promote angiogenesis. Although this study alone will

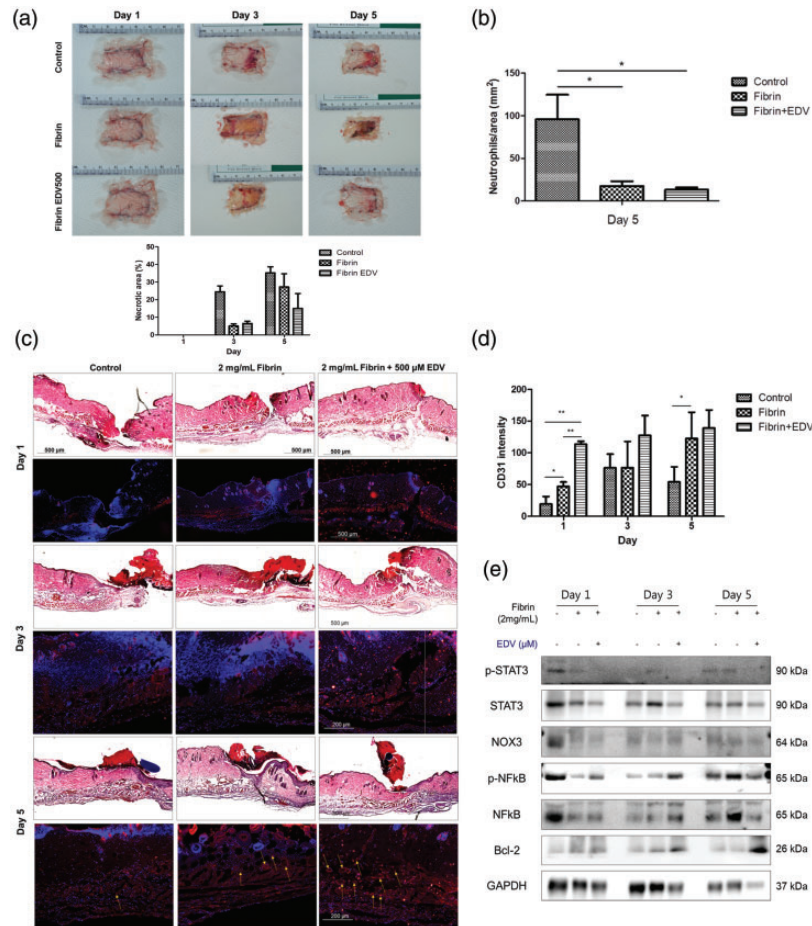


Figure 4. The protective effect of edaravone on wound healing in a DM mouse model. (a) After wounds were created on the backs of mice with streptozotocin-induced diabetes, the percentage of the necrotic areas of the control, fibrin, and EDV with fibrin groups was compared one, three, and five days postoperatively. (b) After wound creation in diabetic mice, neutrophils/area (mm²) of the control, fibrin, and EDV with fibrin groups were compared five days postoperatively. (c) On postoperative days 1, 3, and 5, the H&E-stained cross-sections of the wounds in the control, 2 mg/mL fibrin, and 500 μM EDV with 2 mg/mL fibrin group were compared. (d) To determine the effect of EDV on the vascularity of the wound healing, CD31 staining was used to compare the control, 2 mg/mL fibrin, and 500 μM EDV with 2 mg/mL fibrin groups on days 1, 3, and 5 postoperatively. (e) The ratio of p-STAT3, STAT3, NOX3, p-NF-κB, NF-κB, and bcl-2 was calculated by Western blot analysis in the control, 2 mg/mL fibrin, 500 μM EDV with 2 mg/mL fibrin group on one, three, and five days after wound creation. (A color version of this figure is available in the online journal.)

not be enough to resolve the issues of severe and serious wound problems in diabetes, it may help in assisting the recovery of patients. However, further studies and research are needed for its clinical application.

AUTHORS' CONTRIBUTIONS

All authors participated in the design, interpretation of the studies and analysis of the data and review of the manuscript; HYL, JYJ, and HRL conducted the experiments, YSK wrote the manuscript, and YSS and CHK contributed whole study concept design and management.

DECLARATION OF CONFLICTING INTERESTS

The author(s) declared no conflicts of interest with respect to the research, authorship, and publication of this article.

ETHICAL APPROVAL

Human dermal fibroblast was isolated from human foreskin who gave written informed consent for use of their excised

tissue for academic research which was approved by the Institutional Review Board of Ajou University Hospital (AJIRB-GEN-GEN-12-107) and conducted in accordance with the approved human ethics guidelines.

FUNDING

This study was supported by research Grants from Basic Science Research Program through the National Research Foundation of Korea (NRF) funded by the Ministry of Education, Science and Technology (NRF-2018R1D1A1A02043691).

ORCID ID

Yoo S Shin <https://orcid.org/0000-0002-2007-1100>

REFERENCES

- Saeedi P, Petersohn I, Salpea P, Malanda B, Karuranga S, Unwin N, Colagiuri S, Guariguata L, Motala AA, Ogurtsova K, Shaw JE, Bright D, Williams R, Committee IDFDA. Global and regional diabetes prevalence estimates for 2019 and projections for 2030 and 2045: results

- from the international diabetes federation diabetes atlas, 9(th) edition. *Diabetes Res Clin Pract* 2019;**157**:107843
2. Pihlajaniemi T, Myllyla R, Kivirikko KI, Tryggvason K. Effects of streptozotocin diabetes, glucose, and insulin on the metabolism of type IV collagen and proteoglycan in murine basement membrane-forming EHS tumor tissue. *J Biol Chem* 1982;**257**:14914–20
 3. Gonzalez AC, Costa TF, Andrade ZA, Medrado AR. Wound healing – a literature review. *An Bras Dermatol* 2016;**91**:614–20
 4. Franzen L, Adamson P, Norrby K. Increased angiogenesis during wound healing in rats with streptozotocin-diabetes. *Int J Microcirc Clin Exp* 1990;**9**:401–10
 5. Tecilazich F, Dinh TL, Veves A. Emerging drugs for the treatment of diabetic ulcers. *Expert Opin Emerg Drugs* 2013;**18**:207–17
 6. Dunnill C, Patton T, Brennan J, Barrett J, Dryden M, Cooke J, Leaper D, Georgopoulos NT. Reactive oxygen species (ROS) and wound healing: the functional role of ROS and emerging ROS-modulating technologies for augmentation of the healing process. *Int Wound J* 2017;**14**:89–96
 7. Eble JA, de Rezende FF. Redox-relevant aspects of the extracellular matrix and its cellular contacts via integrins. *Antioxid Redox Signal* 2014;**20**:1977–93
 8. Toyoda K, Fujii K, Kamouchi M, Nakane H, Arihiro S, Okada Y, Ibayashi S, Iida M. Free radical scavenger, edaravone, in stroke with internal carotid artery occlusion. *J Neurol Sci* 2004;**221**:11–7
 9. Won HR, Seo C, Lee HY, Roh J, Kim CH, Jang JY, Shin YS. An important role of macrophages for wound margin regeneration in a murine flap model. *Tissue Eng Regen Med* 2019;**16**:667–74
 10. Hwang JY, Yadav AK, Jang BC, Kim YC. Antioxidant and cytoprotective effects of stachys riedereri var. japonica ethanol extract on UVA irradiated human dermal fibroblasts. *Int J Mol Med* 2019;**43**:1497–504
 11. Chatterjee N, Yang J, Kim HM, Jo E, Kim PJ, Choi K, Choi J. Potential toxicity of differential functionalized multiwalled carbon nanotubes (MWCNT) in human cell line (BEAS2B) and *Caenorhabditis elegans*. *J Toxicol Environ Health A* 2014;**77**:1399–408
 12. Navarro M, del Valle S, Martinez S, Zeppetelli S, Ambrosio L, Planell JA, Ginebra MP. New macroporous calcium phosphate glass ceramic for guided bone regeneration. *Biomaterials* 2004;**25**:4233–41
 13. Liu J, Zhang D, Luo W, Yu J, Li J, Yu Y, Zhang X, Chen J, Wu XR, Huang C. E3 ligase activity of XIAP RING domain is required for XIAP-mediated cancer cell migration, but not for its RhoGDI binding activity. *PLoS One* 2012;**7**:e35682
 14. Lee D, Park S, Bae S, Jeong D, Park M, Kang C, Yoo W, Samad MA, Ke Q, Khang G, Kang PM. Hydrogen peroxide-activatable antioxidant prodrug as a targeted therapeutic agent for ischemia-reperfusion injury. *Sci Rep* 2015;**5**:16592
 15. Zhang GW, Gu TX, Sun XJ, Wang C, Qi X, Wang XB, Li-Ling J. Edaravone promotes activation of resident cardiac stem cells by transplanted mesenchymal stem cells in a rat myocardial infarction model. *J Thorac Cardiovasc Surg* 2016;**152**:570–82
 16. Deeds MC, Anderson JM, Armstrong AS, Gastineau DA, Hiddinga HJ, Jahangir A, Eberhardt NL, Kudva YC. Single dose streptozotocin-induced diabetes: considerations for study design in islet transplantation models. *Lab Anim* 2011;**45**:131–40
 17. Lee MS, Ahmad T, Lee J, Awada HK, Wang Y, Kim K, Shin H, Yang HS. Dual delivery of growth factors with coacervate-coated poly(lactic-co-glycolic acid) nanofiber improves neovascularization in a mouse skin flap model. *Biomaterials* 2017;**124**:65–77
 18. Toutain CE, Brouchet L, Raymond-Letron I, Vicendo P, Berges H, Favre J, Fouque MJ, Krust A, Schmitt AM, Chambon P, Gourdy P, Arnal JF, Lenfant F. Prevention of skin flap necrosis by estradiol involves reperfusion of a protected vascular network. *Circ Res* 2009;**104**:245–54, 12p following 54
 19. Park JK, Kim YS, Kang SU, Lee YS, Won HR, Kim CH. Nonthermal atmospheric plasma enhances myoblast differentiation by eliciting STAT3 phosphorylation. *FASEB J* 2019;**33**:4097–106
 20. Chigurupati S, Arumugam TV, Son TG, Lathia JD, Jameel S, Mughal MR, Tang SC, Jo DG, Camandola S, Giunta M, Rakova I, McDonnell N, Miele L, Mattson MP, Poozala S. Involvement of notch signaling in wound healing. *PLoS One* 2007;**2**:e1167
 21. Wang C, Cai Y, Zhang Y, Xiong Z, Li G, Cui L. Local injection of deferoxamine improves neovascularization in ischemic diabetic random flap by increasing HIF-1alpha and VEGF expression. *PLoS One* 2014;**9**:e100818
 22. Nouvong A, Ambrus AM, Zhang ER, Hultman L, Collier HA. Reactive oxygen species and bacterial biofilms in diabetic wound healing. *Physiol Genom* 2016;**48**:889–96
 23. Kunkemoeller B, Kyriakides TR. Redox signaling in diabetic wound healing regulates extracellular matrix deposition. *Antioxid Redox Signal* 2017;**27**:823–38
 24. Loots MA, Lamme EN, Zeegelaar J, Mekkes JR, Bos JD, Middelkoop E. Differences in cellular infiltrate and extracellular matrix of chronic diabetic and venous ulcers versus acute wounds. *J Invest Dermatol* 1998;**111**:850–7
 25. Hoffman RP. Hyperglycemic endothelial dysfunction: does it happen and does it matter? *J Thorac Dis* 2015;**7**:1693–5
 26. Deveci M, Gilmont RR, Dunham WR, Mudge BP, Smith DJ, Marcelo CL. Glutathione enhances fibroblast collagen contraction and protects keratinocytes from apoptosis in hyperglycaemic culture. *Br J Dermatol* 2005;**152**:217–24
 27. Xuan YH, Huang BB, Tian HS, Chi LS, Duan YM, Wang X, Zhu ZX, Cai WH, Zhu YT, Wei TM, Ye HB, Cong WT, Jin LT. High-glucose inhibits human fibroblast cell migration in wound healing via repression of bFGF-regulating JNK phosphorylation. *PLoS One* 2014;**9**:e108182
 28. Lamers ML, Almeida ME, Vicente-Manzanares M, Horwitz AF, Santos MF. High glucose-mediated oxidative stress impairs cell migration. *PLoS One* 2011;**6**:e22865
 29. Yevdokimova NY. High glucose-induced alterations of extracellular matrix of human skin fibroblasts are not dependent on TSP-1-TGFbeta1 pathway. *J Diabetes Complicat* 2003;**17**:355–64
 30. Watanabe T, Tahara M, Todo S. The novel antioxidant edaravone: from bench to bedside. *Cardiovasc Ther* 2008;**26**:101–14
 31. Yoshida H, Yanai H, Namiki Y, Fukatsu-Sasaki K, Furutani N, Tada N. Neuroprotective effects of edaravone: a novel free radical scavenger in cerebrovascular injury. *CNS Drug Rev* 2006;**12**:9–20
 32. Yuan Y, Zha H, Rangarajan P, Ling EA, Wu C. Anti-inflammatory effects of edaravone and scutellarin in activated microglia in experimentally induced ischemia injury in rats and in BV-2 microglia. *BMC Neurosci* 2014;**15**:125
 33. Emekli-Alturfan E, Alev B, Tunali S, Oktay S, Tunali-Akbay T, Ozturk LK, Yanardag R, Yarat A. Effects of edaravone on cardiac damage in valproic acid induced toxicity. *Ann Clin Lab Sci* 2015;**45**:166–72
 34. Enomoto M, Endo A, Yatsushige H, Fushimi K, Otomo Y. Clinical effects of early edaravone use in acute ischemic stroke patients treated by endovascular reperfusion therapy. *Stroke* 2019;**50**:652–8
 35. Varatharajan R, Lim LX, Tan K, Tay CS, Teoh YL, Akhtar SS, Rupeshkumar M, Chung I, Abdullah NA, Banik U, Dhanaraj SA, Balakumar P. Effect of edaravone in diabetes mellitus-induced nephropathy in rats. *Korean J Physiol Pharmacol* 2016;**20**:333–40
 36. Tsounapi P, Saito M, Dimitriadis F, Koukos S, Shimizu S, Satoh K, Takenaka A, Sofikitis N. Antioxidant treatment with edaravone or taurine ameliorates diabetes-induced testicular dysfunction in the rat. *Mol Cell Biochem* 2012;**369**:195–204
 37. Loomans CJ, de Koning EJ, Staal FJ, Rookmaaker MB, Verseyden C, de Boer HC, Verhaar MC, Braam B, Rabelink TJ, van Zonneveld AJ. Endothelial progenitor cell dysfunction: a novel concept in the pathogenesis of vascular complications of type 1 diabetes. *Diabetes* 2004;**53**:195–9
 38. Naito R, Nishinakamura H, Watanabe T, Nakayama J, Kodama S. Edaravone, a free radical scavenger, accelerates wound healing in diabetic mice. *Wounds* 2014;**26**:163–71
 39. Koizumi T, Tanaka H, Sakaki S, Shimazaki S. The therapeutic efficacy of edaravone in extensively burned rats. *Arch Surg* 2006;**141**:992–5
 40. Hoeldtke RD, Bryner KD, McNeill DR, Hobbs GR, Baylis C. Peroxynitrite versus nitric oxide in early diabetes. *Am J Hypertens* 2003;**16**:761–6
 41. Devaraj S, Cheung AT, Jialal I, Griffen SC, Nguyen D, Glaser N, Aoki T. Evidence of increased inflammation and microcirculatory

- abnormalities in patients with type 1 diabetes and their role in micro-vascular complications. *Diabetes* 2007;**56**:2790–6
42. Pickup JC. Inflammation and activated innate immunity in the pathogenesis of type 2 diabetes. *Diabetes Care* 2004;**27**:813–23
 43. Kaur P, Choudhury D. Insulin promotes wound healing by inactivating NF κ B β 50/P65 and activating protein and lipid biosynthesis and alternating pro/anti-inflammatory cytokines dynamics. *Biomol Concepts* 2019;**10**:11–24
 44. Iwata H, Soga Y, Meguro M, Yoshizawa S, Okada Y, Iwamoto Y, Yamashita A, Takashiba S, Nishimura F. High glucose up-regulates lipopolysaccharide-stimulated inflammatory cytokine production via c-jun N-terminal kinase in the monocytic cell line THP-1. *J Endotoxin Res* 2007;**13**:227–34
 45. Miller AM, Wang H, Bertola A, Park O, Horiguchi N, Ki SH, Yin S, Lafdil F, Gao B. Inflammation-associated interleukin-6/signal transducer and activator of transcription 3 activation ameliorates alcoholic and nonalcoholic fatty liver diseases in interleukin-10-deficient mice. *Hepatology* 2011;**54**:846–56
 46. Chen Y, Wang JJ, Li J, Hosoya KI, Ratan R, Townes T, Zhang SX. Activating transcription factor 4 mediates hyperglycaemia-induced endothelial inflammation and retinal vascular leakage through activation of STAT3 in a mouse model of type 1 diabetes. *Diabetologia* 2012;**55**:2533–45
 47. Gurzov EN, Eizirik DL. Bcl-2 proteins in diabetes: mitochondrial pathways of beta-cell death and dysfunction. *Trends Cell Biol* 2011;**21**:424–31
 48. Tuan TL, Song A, Chang S, Younai S, Nimni ME. In vitro fibroplasia: matrix contraction, cell growth, and collagen production of fibroblasts cultured in fibrin gels. *Exp Cell Res* 1996;**223**:127–34
 49. Bensaid W, Triffitt JT, Blanchat C, Oudina K, Sedel L, Petite H. A bio-degradable fibrin scaffold for mesenchymal stem cell transplantation. *Biomaterials* 2003;**24**:2497–502
 50. Bhang SH, Lee TJ, La WG, Kim DI, Kim BS. Delivery of fibroblast growth factor 2 enhances the viability of cord blood-derived mesenchymal stem cells transplanted to ischemic limbs. *J Biosci Bioeng* 2011;**111**:584–9
 51. Saul JM, Linnes MP, Ratner BD, Giachelli CM, Pun SH. Delivery of non-viral gene carriers from sphere-templated fibrin scaffolds for sustained transgene expression. *Biomaterials* 2007;**28**:4705–16
 52. Schek RM, Hollister SJ, Krebsbach PH. Delivery and protection of adenoviruses using biocompatible hydrogels for localized gene therapy. *Mol Ther* 2004;**9**:130–8
 53. Montana M, Tabele C, Curti C, Terme T, Rathelot P, Gensollen S, Vanelle P. Organic glues or fibrin glues from pooled plasma: efficacy, safety and potential as scaffold delivery systems. *J Pharm Pharm Sci* 2012;**15**:124–40
 54. Geer DJ, Swartz DD, Andreadis ST. Fibrin promotes migration in a three-dimensional in vitro model of wound regeneration. *Tissue Eng* 2002;**8**:787–98
 55. Hojo M, Inokuchi S, Kidokoro M, Fukuyama N, Tanaka E, Tsuji C, Miyasaka M, Tanino R, Nakazawa H. Induction of vascular endothelial growth factor by fibrin as a dermal substrate for cultured skin substitute. *Plast Reconstr Surg* 2003;**111**:1638–45
 56. Caiado F, Carvalho T, Silva F, Castro C, Clode N, Dye JF, Dias S. The role of fibrin E on the modulation of endothelial progenitors adhesion, differentiation and angiogenic growth factor production and the promotion of wound healing. *Biomaterials* 2011;**32**:7096–105

(Received July 24, 2020, Accepted October 27, 2020)